

Deposition and characterization of diamond-like carbon thin films by electro-deposition technique using organic liquid

S.C. Ray^{a),b)}

Department of Physics, Tamkang University, Tamsui 251, Taiwan

B. Bose

Department of Physics, North-Bengal University, Siliguri 734430, India

J.W. Chiou, H.M. Tsai, J.C. Jan, Krishna Kumar, and W.F. Pong

Department of Physics, Tamkang University, Tamsui 251, Taiwan

D. DasGupta

Department of Physics, North-Bengal University, Siliguri 734430, India

G. Fanchini and A. Tagliaferro

Dipartimento di Fisica & Unità INFN, Politecnico di Torino Torino, Italy

(Received 5 December 2003; accepted 22 December 2003)

Diamond-like carbon films were synthesized by electro-deposition technique from an organic liquid (a solution of alpha- and beta-pinenes in n-hexane) on silicon substrate at room temperature and at room pressure. The x-ray diffraction (XRD), Fourier-transform infrared (FTIR) spectra, Raman spectra, photoluminescence (PL), and x-ray absorption near edge structure (XANES) spectra analysis were used to study the properties of the diamond-like carbon (as-deposited and annealed) films. The XRD measurement indicated that the film contains some diamond-crystalline phases whereas Raman spectra did not show any prominent diamond-like peak. PL intensity is higher for the as-deposited film and decreased with high-temperature vacuum annealing. FTIR spectra showed the presence of sp^3 hybridization C–H bonds and their intensity decreases at higher annealing temperature. C and O K-edge XANES spectra showed that π^* (sp^2) intensity significantly decreases when the annealing temperature is 600 °C.

I. INTRODUCTION

Diamond-like carbon (DLC) films have attracted interest for several applications, such as corrosion protective coatings of metal, wear-resistant coatings, and use as optical and electronic components. A large number of different methods, including chemical vapor deposition techniques,¹ ion-beam laser processing techniques,² etc., are used for the preparation of these films. However, we have succeeded in demonstrating a new method for the preparation of those films in an atmospheric pressure and at room temperature. This method is based on an electrochemical process. This is our first attempt to deposit DLC films by this technique using organic compounds, in this case, a solution of alpha- and beta-pinenes in n-hexane. The electro-deposition technique is not widely used for the preparation of DLC films and very few reports were found.^{3–8} In this article, we present the

preparation of the DLC films having thickness 700 nm by an easy and inexpensive electrodeposition technique at room pressures and temperature using organic compounds and discuss their preliminary characterization.

II. EXPERIMENTAL DETAILS

The apparatus used in our experiment is an electrolytic cell system shown in Fig. 1. The films were deposited on silicon (100) wafers with resistivity of 20 Ω cm and size of 10 × 20 × 0.3 mm³. The range of the substrate temperature was 25–35 °C. The substrates (Si) were treated with dilute HNO₃–HF solution for few minutes and then cleaned by ultrasonic treatment before deposition. The electrolysis dc power supply was used, keeping the current density range 2–3 mA/cm². The deposition time ranged from 2 to 5 h. Thickness of the films was in the range between 600 and 800 nm. Films are annealed in vacuum (10^{–5} Torr) in the temperature range 400–600 °C. The films were characterized by x-ray diffraction (XRD), Fourier-transform infrared (FTIR) spectroscopy, thickness profile, Raman, photoluminescence (PL), and x-ray absorption near edge structure (XANES) spectra. Raman spectra as well as PL spectra were performed using a

^{a)}Address all correspondence to this author.

^{b)}Present address: Instituto de Ciencia de Materiales de Madrid, CSIC, Campus de Cantoblanco, E-28049, Madrid, Spain.
e-mail: raysekhar@rediffmail.com

DOI: 10.1557/JMR.2004.0146

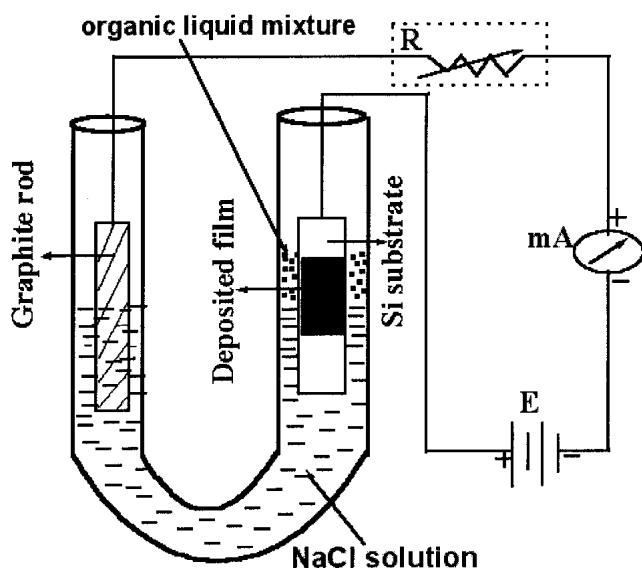


FIG. 1. Schematic diagram of the apparatus for the deposition of DLC films used in our experiment.

Renishaw (Derbyshire, UK) micro-spectrometer, excited by a 2.41 eV Ar^+ laser energy at the laser power of 25 mW with spot area of $3 \mu\text{m}^2$. FTIR transmission measurements were performed using Perkin-Elmer (Osaka, Japan) FT-IR 2000 spectrometer and XRD spectra were performed using PHILIPS (Tokyo, Japan) diffractometer (model PW 1390) with $\text{Cu K}\alpha$ radiation (Ni filter) at 1.54 \AA . The film thickness was measured by a Tenkor (Osaka, Japan) stylus profilometer. XANES spectra of C K and O K-edge were performed using the high-energy spherical grating monochromator (HSGM) at the beam line 20-A with electron-beam energy of 1.5 GeV and maximum stored current of 200 mA at the National Synchrotron Radiation Research Center (NSRRC), Hsinchu, Taiwan. The data were collected in the total yield mode by recording the sample drain current mode. Simultaneously, the signal from a gold grid located upstream in the x-ray path was recorded, and the spectra were used for normalization after pre-edge background subtraction. A second normalization was performed by keeping the area fixed under the spectra in the energy range (315–335 eV for C K-edge and 552–569 eV for O K-edge). A reference spectrum was measured from a standard type; a highly oriented pyrolytic graphite (HOPG) sample and MoO_3 sample were used for energy calibration for all films of C K-edge spectra and O K-edge spectra respectively. All samples were out-gassed in vacuum (10^{-9} Torr) to about $150 \text{ }^\circ\text{C}$ prior to the XANES measurements to eliminate the surface contamination. All measurement was taken at room temperature.

Deposition process and mechanism

In the deposition process we chose a U-tube with a graphite rod in one side and silicon wafer (substrate) is in

other side of the tube, which acted as a cathode and anode respectively. The distance between the electrodes was 7 mm. Due to similar lattice structure of diamond, a silicon wafer (100) was used as a substrate for the deposition of DLC films. To ensure adequate electrical conductance of the electrode, *p*-type doped silicon with conductivity of 0.05 S cm^{-1} was used. The mixture of organic compounds described above served as the carbon source for the deposition of DLC films. Sodium chloride solution was used in one-third of the tube, and the organic liquid mixture was poured on the top of the electrolyte (sodium chloride solution) at the anode side (see Fig. 1) so the silicon substrate dipped partially in both the electrolyte as well as the organic solution. In the film-forming process, chlorine liberated at the anode attacked the hydrocarbon(s) to combine with the hydrogen and release carbon, which was deposited on the substrate. Details of the mechanism are not exactly known at present. Various hydrocarbons and their combination have been tried, but the best films in terms of rate of deposition, adhesion to the substrate, and uniformity were obtained with a mixture of alpha-pinene, beta-pinene, and normal hexane (typical ratio 1:1:10 by volume, although this is not critical), and the results for these are reported here.

III. RESULTS AND DISCUSSION

A. XRD study

At a visual analysis, the films are homogeneous and shiny silver-golden in color. The films were inert to heavy acid and alkalis and did not dissolve in organic solvents. XRD spectra show that they contain few diamond peaks in the film as deposited as well as annealed films. Figure 2 shows the XRD spectra of as-deposited film and that annealed at $600 \text{ }^\circ\text{C}$. The peaks observed at $2\theta = 38.69^\circ, 44.95^\circ, 82.55^\circ, 88.43^\circ,$ and 98.44° are assigned to the reflection of diamond.^{4,6,9–13} A feature is observed for as-deposited films in the diffraction pattern around $2\theta = 13.30^\circ$ and 12.56° for the film annealed at $600 \text{ }^\circ\text{C}$. These two peaks are assigned to (001) and (300) diffraction peak of disordered graphite respectively. The reticular distances $d_{001} = 0.665 \text{ nm}$ and $d_{300} = 0.704 \text{ nm}$ correspond to the interplanar distances between two adjacent sheets in graphitized carbons.^{11,14} Apart from those peaks other few peaks were observed and is due to SiO_2 and Si substrate. The peak position d and hkl values and their assignment are listed in Table I(a) along with the associated references. It shows that in annealing at $600 \text{ }^\circ\text{C}$, the number of diamond peaks more, which reveals that the crystallinity increases with annealing temperatures, and is consistent with the XANES spectra (discussed in Sec. III D).

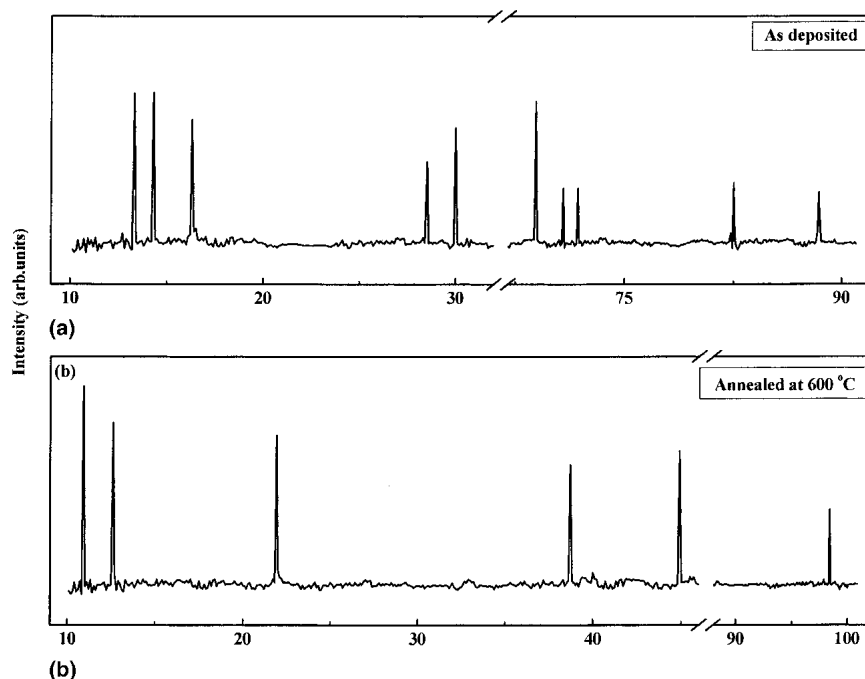


FIG. 2. XRD patterns of the DLC films: (a) as deposited and (b) annealed at 600 °C.

TABLE I(a). Lattice spacing values for electro-deposited DLC film obtained from XRD.

| Films | Present work | | Previous work | | Assignment | |
|--------------------|--------------------|--------|---------------|-----------|------------------|--------------|
| | Peak position (2θ) | d (nm) | d (nm) | Reference | Diamond/graphite | <i>h k l</i> |
| As deposited | 13.30 | 0.665 | 0.668 | 9 | Graphite | 0 0 1 |
| | 14.32 | 0.618 | 0.618 | 10 | SiO ₂ | 0 2 0 |
| | 16.27 | 0.544 | 0.545 | 9 | Carbon cluster | ... |
| | 28.54 | 0.312 | 0.313 | 11 | Si | 1 1 1 |
| | 30.01 | 0.297 | 0.307 | 9 | SiO ₂ | 2 0 0 |
| | 68.88 | 0.136 | 0.136 | 6, 11 | Si | 4 0 0 |
| | 70.81 | 0.133 | 0.132 | 9 | Si | 1 0 0 |
| | 71.86 | 0.131 | 0.131 | 10 | SiO ₂ | 4 2 1 |
| | 82.55 | 0.117 | 0.116 | 12 | Diamond | 1 0 3 |
| | 88.43 | 0.110 | 0.109 | 12 | Diamond | 2 0 0 |
| Annealed at 600 °C | 10.91 | 0.810 | 0.810 | 13 | SiO ₂ | 1 0 1 |
| | 12.56 | 0.704 | 0.668 | 11 | Graphite | 3 0 0 |
| | 21.93 | 0.405 | 0.406 | 9 | Carbon cluster | ... |
| | 38.69 | 0.233 | 0.240 | 4 | Diamond | 1 1 0 |
| | 44.95 | 0.201 | 0.201 | 4 | Diamond | 1 1 1 |
| | 98.44 | 0.102 | 0.104 | 4 | Diamond | 2 2 2 |

TABLE I(b). Raman spectra analysis and photoluminescence results of electro-deposited DLC film.

| Films | Raman spectra analysis | | | | | Photoluminescence (PL) | | |
|-------------------|-----------------------------------|----------------|--------------------------------|----------------|--|---------------------------|--------------|-----------------|
| | Peak position (cm ⁻¹) | | Peak width (cm ⁻¹) | | Int. ratio (I _D /I _G) | PL Int. (arbitrary units) | Peak at (eV) | Peak width (eV) |
| | w _D | w _G | τ _D | τ _G | | | | |
| As deposited | 1369 | 1595 | 212 | 94 | 0.61 | 14915 | 1.83 | 0.33 |
| Annealed (400 °C) | 1371 | 1599 | 236 | 82 | 0.75 | 164 | 1.88 | 0.35 |
| Annealed (600 °C) | 1367 | 1602 | 256 | 73 | 0.81 | 68 | 1.87 | 0.44 |

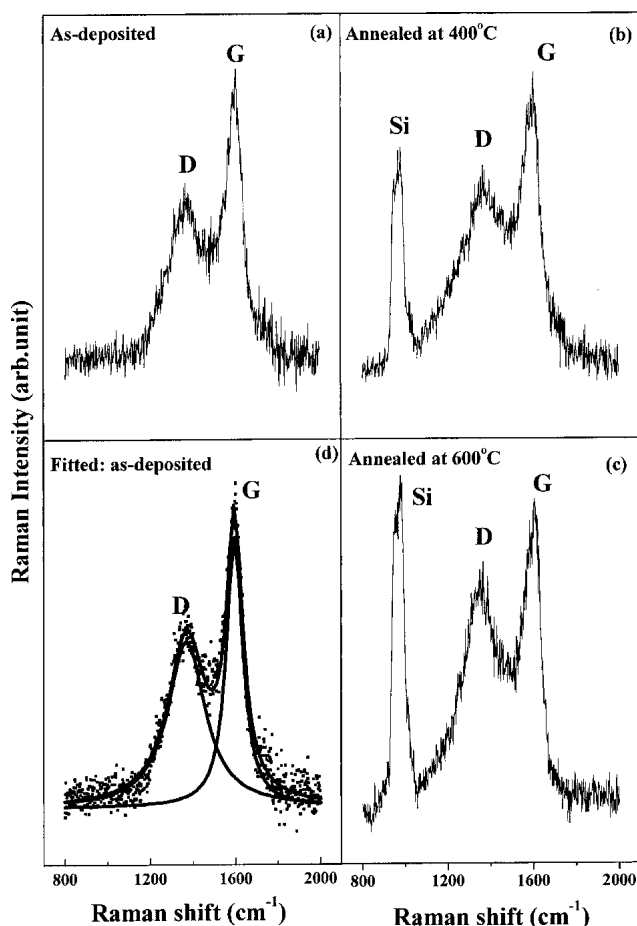


FIG. 3. Raman spectra of the DLC films: (a) as deposited, (b) annealed at 400 °C, (c) annealed at 600 °C, and (d) decomposition as deposited film into D and G peak using Gaussian fit. (D, disorder; G, graphite; and Si, silicon substrate).

B. Raman spectra and PL study

The Raman spectra of the films (Fig. 3) exhibit the well known disorder-D ($1367\text{--}1371\text{ cm}^{-1}$) and graphite-G ($1595\text{--}1602\text{ cm}^{-1}$) peaks found in both films¹⁵ as deposited as well as annealed film. In annealed films, an extra peak at approximately 950 cm^{-1} was observed and is Si-peak appears due to silicon substrate. The G peak occurs both in olefinic (chains) and aromatic (rings) clusters. In contrast, the D peak is necessarily related to the presence of aromatic rings.^{15,16} Thus, the significant D peak in these films shows that no changes occur in bonding configuration during the annealing stage. The G and D features [Table I(b)] of the electrodeposited films are best fitted (Fig. 3) with two Gaussian curves. In the films, the two Raman parameters the most related to the bonding nature in the sp^2 phase are the I_D/I_G peak intensity ratio and the G-peak position ω_G .¹⁶ ω_G slowly up-shifts during annealing (indicating a small transition to shorter and/or more aligned carbon-carbon bonds¹⁶). The I_D/I_G ratio monotonically increases with

annealing temperature, and this may be ascribed to the increase either in number or in size of the sp^2 clusters. Further information from Raman analysis might be obtained by the G-peak bandwidth τ_G .¹⁶ The values of τ_G are lower at the highest annealing temperatures (i.e., $\tau_G \approx 73 \pm 20\text{ cm}^{-1}$ at 600 °C, to be compared with $\tau_G \approx 94 \pm 20\text{ cm}^{-1}$ for as deposited sample). The I_D/I_G ratio suggests [Table I(b)] a monotonic increase of aromatic clustering in the film consistently with the increase in concentration of the sp^2 clusters or an increase in the sp^2 cluster size. The lowest ω_G values do not necessarily signify a different cluster type, but consistent with the observation of higher G-peak positions in graphitic, may signify that the clusters are embedded in a different environment.

The PL spectra are shown in Fig. 4, indicating that PL intensity decrease and the peak positions of PL peak energy are slightly shifted in higher energy with annealing temperature. The shift of PL peak with temperature, analogous to that shown in Fig. 3, is also typical for a-C films.^{17,18} A similar phenomenon was observed by Xu et al.¹⁹ in a-C:H films grown by plasma-enhanced chemical vapor deposition at different substrate temperatures. It is expected that the photoluminescence is due to the recombination of electron-hole pairs within sp^2 clusters.²⁰ PL intensity is related to the floppiness of the

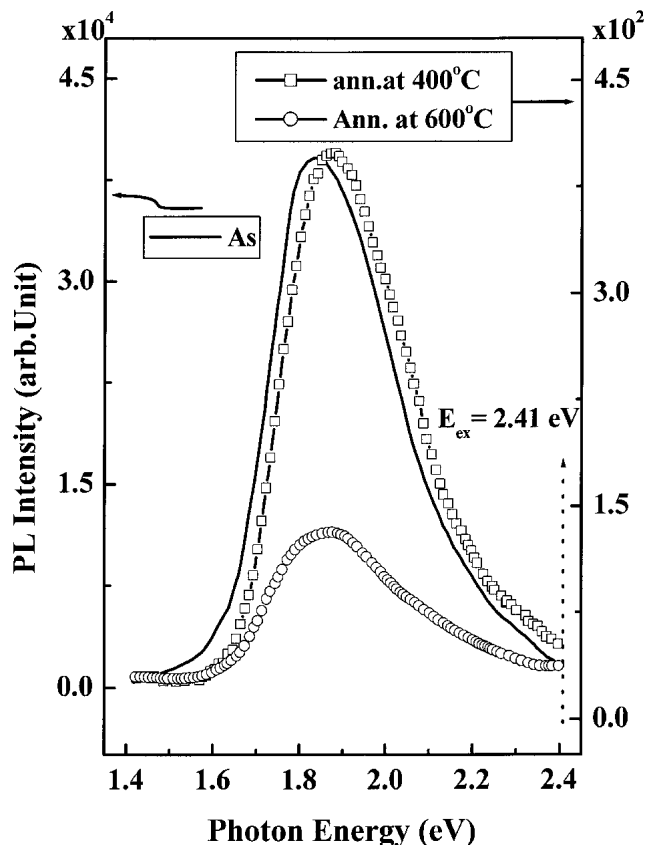


FIG. 4. PL spectra of the DLC as-deposited and annealed at 400 and 600 °C.

films (which quench the density N_d of non-radiative recombination centers) with the presence of an OH group and to the quantum confinement (reducing the capture radius R_0). PL intensity decreases [Table I(b)] at higher vacuum annealing temperature due to compactness of the films²¹ as compactness and OH concentration decrease with annealing.

C. FTIR study

The FTIR spectrum of the as-deposited and annealed (at 400 and 600 °C) films in the frequency range 500–3500 cm^{-1} are reported in Fig. 5 addressing all possible vibration modes.²² The spectrum shows mainly the presence of C–C (at 1220 cm^{-1} and the 1430–1750 cm^{-1} range) and hydrocarbon CH_n (800 cm^{-1} and 2760–3150 cm^{-1} range) inclusions in the film, as expected from the composition of the fluid precursors. In addition, the presence of C–O stretching vibration (near 1050 cm^{-1}) and environmental CO_2 (near 2360 cm^{-1}) are present. It was observed from the spectra that the C–C bond becomes slightly stronger (near 1515 and 1725 cm^{-1}) in the

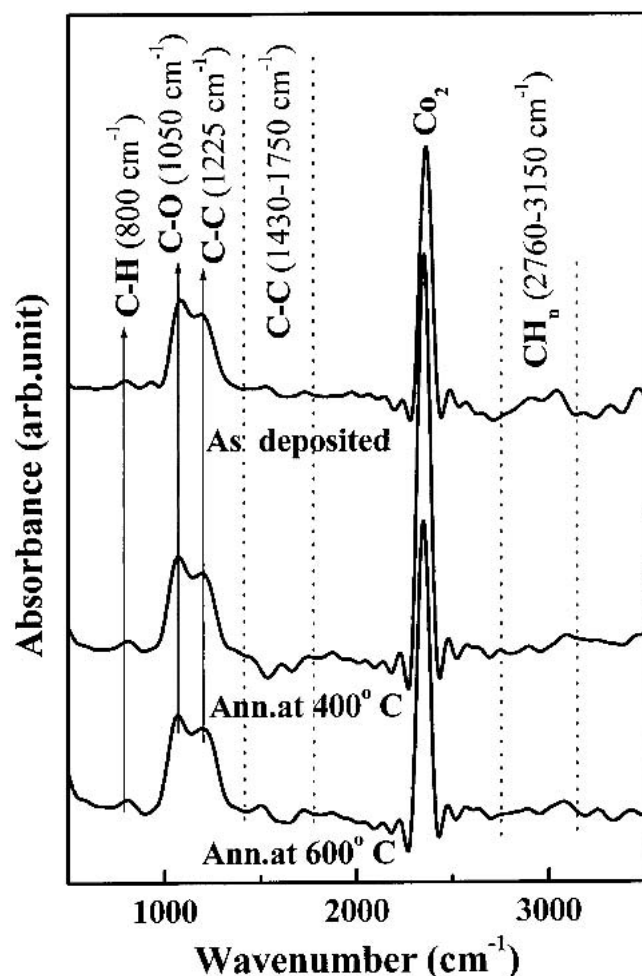


FIG. 5. FTIR spectra of the DLC films as-deposited and annealed at 400 and 600 °C.

range 1430–1750 cm^{-1} (see Fig. 5), whereas the CH_n band become weaker in the range 2760–3150 cm^{-1} (see Fig. 5), when the films are annealed at higher temperature (at 600 °C). The reason may be due to higher temperature removing H atoms from the film surface²³ and the formation of more C–C bonding.

D. XANES spectra analysis

Figure 6 shows the C K-edge XANES spectra of the electrodeposited DLC films, as-deposited and annealed. They are compared to reference XANES spectra of natural diamond, graphite, and HOPG. Most of the structures in the absorption edge of these references can be related to features in the unoccupied density of states.²⁴ The peak at 285.5 eV is assigned, from its polarization dependence, as a $1s \rightarrow \pi^*$ transition corresponding to anti-bonding states of unsaturated carbons.²⁴ The energy of this transition is in close agreement with the C 1s core-level energy at 285.6 eV in HOPG and at 285.4 eV in the graphite reference.^{24,25} Therefore, it is quite representative of the occurrence of unsaturated bonds, which are intense in HOPG and graphite. As shown in Fig. 6, the XANES spectrum of the DLC films displayed the

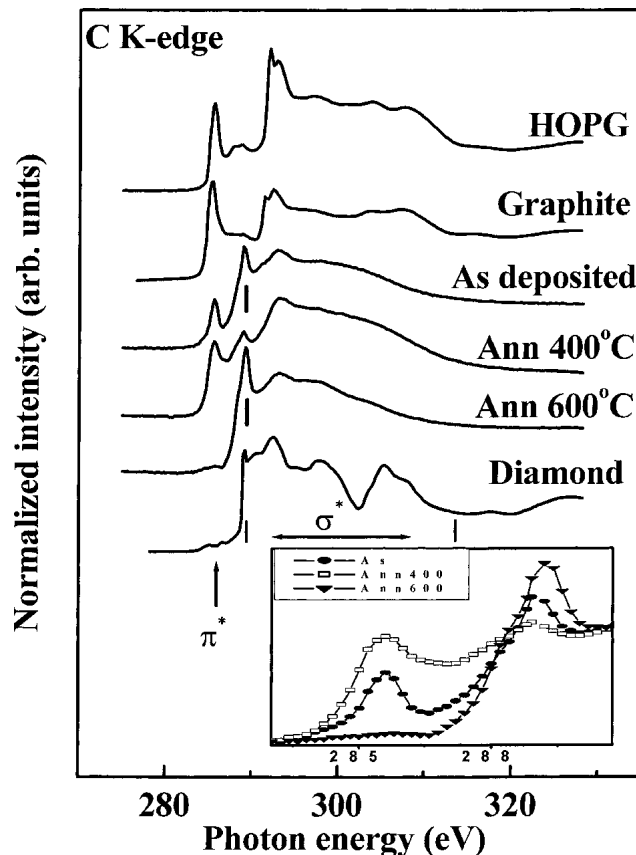


FIG. 6. Normalized C K-edge absorption spectra of DLC films. (inset) Magnified π^* region of C K-edge absorption spectra.

first edge jump at 289 eV (shown using vertical line in Fig. 6) corresponds to the threshold of $1s \rightarrow \sigma^*$ transitions followed by a wide peak at 293 eV and a wide broad peak in the range 295–312 eV. The contributions ranging within 290–312 eV labeled σ^* correspond to the transitions of the C $1s$ core elements to C–C anti-bonding states σ^* (HOPG) or to empty density of states with σ symmetry. The different features observed in the XANES spectrum were previously reported^{24,25} and associated with electronic dipole transitions from the C($1s$) core level to unoccupied states above the Fermi level in the diamond crystal field. In particular, the sharp peak at 289 eV is associated with a core excitation.^{24,25} The intensity of the π^* (sp^2) region of 600 °C annealed film undergoes a significant decrease and simultaneous increase of σ^* threshold intensity at 289 eV [inset Fig. 6], which indicates the formation of sp^3 -rich DLC films and is consistent with the XRD spectra shown in Fig. 2(b).

Photo absorption spectra from the O ($1s$) core level are shown in Fig. 7 and reveal that a small amount of oxygen is present in the sample. When the annealing temperature is comparatively higher (600 °C), it is no longer detectable. A similar phenomenon was observed by

Jiménez et al.^{24,25} during annealing of the boron carbide films. The presence of a peak at approximately 531.2 eV (more clearly shown in inset in Fig. 7) $\pi^*_{C=O}$ levels is predicted in a localized, non-interacting description of the π^* electronic structure.²⁶ These might be expected to be probable quasi-degenerate because of the large spatial separation.²⁶ The presence of $\sigma^*_{C=O}$ resonance is strongly dominated by the broad resonance peak center at 539 eV shown in Fig. 7, occurring where expected from the bond length correlation.²⁶ The similar peak in the C ($1s$) near edge x-ray absorption fine structure has been reported in several previous studies of carbon systems and identified as carbon nanotubes features,²⁷ graphite interlayer states,²⁸ or the σ^* exciton of amorphous carbon.²⁹ Our assignment of these features to some C=O moiety is commensurate with the O ($1s$) XANES in all the samples studied and consistent with the decrease of the features in the C ($1s$) and O ($1s$) spectra due to formation of DLC films.

IV. CONCLUSION

This work represents our first attempts to demonstrate that the electrodeposited technique can be used to deposit diamond-like amorphous carbon films on silicon substrates using a mixture of organic liquid compounds as starting materials at room pressure and temperature. XRD measurement confirmed the presence of diamond-crystalline phases but Raman spectra did not show any such evidence. PL intensity is higher for the as-deposited film and decreases at higher temperature vacuum annealing. FTIR spectra show the presence of sp^3 hybridization C–H bonds and decrease at high temperature annealing, becoming more compact and C–C connective films. C and O K-edge XANES spectra show that π^* (sp^2) intensity significantly decreases and provides further evidence for the compactness of the films when the annealing temperature is 600 °C. At this temperature, significant decrease of the intensity of the π^* (sp^2) region and increase of the intensity at σ^* (sp^3) threshold at approximately 289 eV in C K-edge confirm the formation of sp^3 -rich DLC film. This technique is a very simple and low-cost method, which requires no sophisticated specialized setup. Coating large surfaces by means of this technique is even cheaper than plasma techniques. Another advantage is the ease of coating both sides of the substrate instead only one with an otherwise inaccessible surface. Further work for understanding the deposition mechanism of chemistry process for formation of film structure. This would help in optimizing the various parameters, along with the best choice of substrate and combination of compounds as starting materials so films of a superior quality can be obtained.

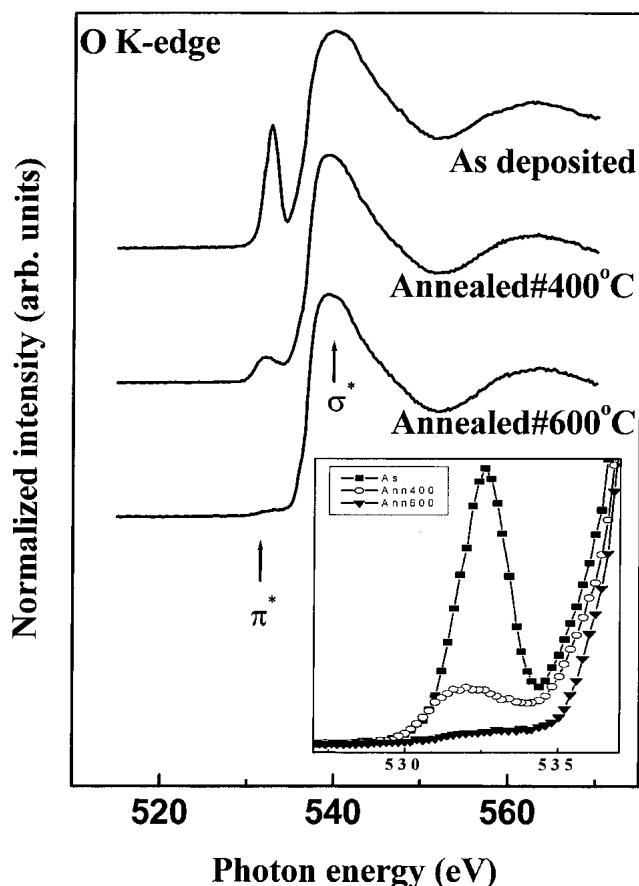


FIG. 7. Normalized O K-edge absorption spectra of DLC films. (inset) Magnified π^* region of O K-edge absorption spectra.

REFERENCES

1. J.C. Angus and C.C. Hayman, *Science* **241**, 914 (1988).
2. A.A. Voevodin, S.J.P. Laube, S.D. Walck, J.S. Solomon, M.S. Donley, and J.S. Zabinski, *J. Appl. Phys.* **78**, 4123 (1995).
3. H. Wang, M.R. Shen, Z.Y. Ning, C. Ye, C.B. Cao, H.Y. Dang, and H.S. Zhu, *Appl. Phys. Lett.* **69**, 1074 (1996).
4. V.P. Novikov and V.P. Dymont, *Appl. Phys. Lett.* **70**, 200 (1997).
5. H. Wang, M.R. Shen, Z.Y. Ning, C. Ye, H.Y. Dang, C.B. Cao, and H.S. Zhu, *Thin Solid Films*. **293**, 87 (1997).
6. Q. Fu, J.T. Jiu, H. Wang, C.B. Cao, and H.S. Zhu, *Chem. Phys. Lett.* **301**, 87 (1999).
7. D. Guo, K. Cai, L. Li, and H. Zhu, *Chem. Phys. Lett.* **325**, 499 (2000).
8. A.M. Chen, C. Pingsuthiwong, and T.D. Golden, *J. Mater. Res.* **18**, 1561 (2003).
9. K. Asokan, S.K. Srivastava, D. Kabiraj, S. Mookerjee, D.K. Avasthi, J.C. Jan, J.W. Chiou, W.F. Pong, L.C. Ting, and F.Z. Chien, *Nucl. Instrum. Meth. Phys. Res. B.* **193**, 324 (2002).
10. S. Gibbs, *Z. Kristallogr.* **145**, 108,(1977).
11. Powder x-ray diffraction data of elements, oxides and minerals for high pressure XRD experiments by Masami Kanzaki, (2000).
12. P. Darrell, Y. Xi, and L. Jenq, *J. Am. Ceram. Soc.* **75**, 1876 (1992).
13. S. Ono, *Science* **282**, 720 (1998).
14. L. Fayette, B. Marcus, M. Mermoux, G. Tourillon, K. Laffon, P. Parent, and F. Le Normand, *Phys. Rev. B.* **57**, 14123 (1998).
15. R.O. Dillon, J.A. Woollam, and V. Katkanat, *Phys. Rev. B.* **29**, 3482 (1994).
16. A.C. Ferrari and J. Robertson, *Phys. Rev. B.* **61**, 14095 (2000).
17. G.A.J. Rusli, Amaratunga, and J. Robertson. *Phys.Rev. B* **53**, 16306 (1996).
18. R.A. Street, *Adv. Phys.* **25**, 397 (1976).
19. S. Xu, T. Ma, W. Li, K. Chen, J. Du, X. Huang, and J. Non-Cryst. Solids **266-269**, 769 (2000).
20. F. Demichelis, S. Schreiter, and A. Tagliaferro, *Phys. Rev. B* **51**, 2134 (1995).
21. G. Fanchini, S.C. Ray, A. Tagliaferro, and E. Laurenti, *J. Phys. Condens. Matter.* **14**, 13231 (2002).
22. N.B. Colthup, *Introduction to Infrared Spectroscopy* (Academic, Boston, MA, 1990).
23. J.V. Anguita, S.R.P. Silva, A.P. Burden, B.J. Sealy, S. Haq, M. Hebron, I. Sturland, and A. Prichard, *J. Appl. Phys.* **86**, 6276 (1999).
24. M.M. Gracia, I. Jiménez, L. Vázquez, C. Gómez-Aleixandre, J.M. Albella, L.J. Terminello, and F.J. Himpsel, *Appl. Phys. Lett.*, **72** 2105 (1998).
25. R. Gago, I. Jiménez and J.M. Albella, *Surf. Sci.* **482-485**, 530 (2001).
26. J.T. Francis and A.P. Hitchcock, *J. Phys. Chem.* **96**, 6598 (1992).
27. M. Imamura, H. Shimada, N. Matsubayashi, M. Yumura, K. Uchida, S. Oshima, Y. Kuriki, Y. Yoshimura, T. Sato and A. Nishijima, *Jpn. J. Appl. Phys. Part 1*, **33**, L1017 (1994).
28. D.A. Fischer, R.M. Wentzcovitch, R.G. Carr, A. Continenza, and A.J. Freeman, *Phys. Rev.B* **44**, 1427 (1991).
29. A. Gutiérrez and M.F. López, *Europhys. Lett.* **31**, 1427 (1995).